

Mechanistic evidence for a front-side, S_{N_i} -type reaction in a retaining glycosyltransferase

Seung Seo Lee¹, Sung You Hong^{1,3}, James C Errey¹, Atsushi Izumi², Gideon J Davies² & Benjamin G Davis^{1*}

A previously determined crystal structure of the ternary complex of trehalose-6-phosphate synthase identified a putative transition state-like arrangement based on validoxylamine A 6'-O-phosphate and uridine diphosphate in the active site. Here linear free energy relationships confirm that these inhibitors are synergistic transition state mimics, supporting front-face nucleophilic attack involving hydrogen bonding between leaving group and nucleophile. Kinetic isotope effects indicate a highly dissociative oxocarbenium ion-like transition state. Leaving group ¹⁸O effects identified isotopically sensitive bond cleavages and support the existence of a hydrogen bond between the nucleophile and departing group. Brønsted analysis of nucleophiles and Taft analysis highlight participation of the nucleophile in the transition state, also consistent with a front-face mechanism. Together, these comprehensive, quantitative data substantiate this unusual enzymatic reaction mechanism. Its discovery should prompt useful reassessment of many biocatalysts and their substrates and inhibitors.

Glycosyltransferases are among the most important enzymes in the field of glycobiology. They are responsible for the biosynthesis of glycans and glycoconjugates, which play a vital role in signaling, recognition, pathogenesis and bacterial cell wall formation¹. However, the catalytic mechanism of glycosyltransferases that utilize nucleoside diphosphate sugars (for example, UDP-glucose and GDP-mannose) remains mostly unclear¹. Inverting glycosyltransferases are suggested to use a single-displacement mechanism with an oxocarbenium ion-like transition state and an asynchronous S_{N2} mechanism, characteristics that are supported by several mechanistic studies and kinetic isotope effects measurements^{2,3} as well as by numerous three-dimensional structures¹. The reactions of the glycosyltransferases that result in the retention of stereochemistry at the anomeric center (retaining glycosyltransferases) are especially poorly understood; in contrast to those with inverting glycosyltransferases, the kinetic and structural studies of retaining glycosyltransferases have not provided unambiguous evidence for their mode of action¹. With analogy to the double-displacement mechanism of retaining glycoside hydrolases⁴ that involves the formation of a covalent intermediate with configurational inversion followed by the hydrolysis of the intermediate with another inversion, it is suggested that the retaining glycosyltransferases follow a double-displacement mechanism. However, many data are at odds with the double-displacement pathway. For instance, although some elegant experiments using mutant enzymes are able to highlight intermediates^{5,6} (for example, on distant nucleophiles⁵) or perform chemical rescue⁷, attempts to trap the covalent glycosyl-enzyme intermediate and other types of relevant intermediates in wild-type enzymes have been unsuccessful^{5,8}. Moreover, a long list^{9–15} (see also **Supplementary Results, Supplementary Fig. 1**) of structural data on retaining glycosyltransferases exists that suggests that few have amino acid side chains suitably positioned to act as a nucleophile in the active site in such a mechanism. Amino acid sequence alignments fail to show any consistently conserved amino acid residues for such an important role. In glycoside

hydrolases, where such a mechanism is well documented, the nucleophilic, acidic and basic residues within the enzyme family are essentially invariant¹.

As an alternative possibility, the 'internal return-like' mechanism, also called the S_{N_i} -like mechanism, has been suggested, in which the nucleophilic attacks from the same face as the leaving group departure^{1,10,15}. The concept of a general internal nucleophilic substitution mechanism S_{N_i} (substitution nucleophilic internal), which is neither simply S_{N1} nor S_{N2} , was first invoked to explain unusual stereochemical outcomes of simple alkyl halides¹⁶; this so-called 'Ingold-type' nomenclature focuses on defining transformation type. This mechanism is classically invoked in the characterization of the reactive stereochemical course of secondary alkyl chlorosulfites, which leads to retention when the nucleophile and leaving group are constrained on the same face; importantly, these early studies highlighted that when constraint was removed, attack occurred from the other face. This mechanism is also observed in carbohydrate chemistry. It is directly relevant to our study that such a mechanism for glycosyltransfer was first proposed, in the absence of any enzyme, to explain the retention of anomeric stereochemistry in the solvolysis of α -glucosyl fluoride by mixtures of ethanol and trifluoroethanol¹⁷. Theoretical studies suggest that such an internal return mechanism can provide an energetically plausible pathway inside enzymes as a result of active site geometrical constraints¹⁸. An S_{N_i} -like mechanism is also suggested based on the ternary complex structure of a retaining galactosyltransferase from *Neisseria meningitidis* containing acceptor and donor substrate analogs and the kinetic study of mutants¹⁰. A series of reports on an archetypal, non-Leloir glycosyltransferase, trehalose phosphorylase, have postulated, on the basis of kinetic data, that this unusual mechanism might be operating^{19,20}. A recent study suggests that a change in kinetic and chemical mechanism—that is, a shift from a double-displacement to a sequential 'front-side' mechanism—takes place when a retaining glycosidase, sucrose phosphorylase, is engineered to possess synthetic activity²¹. Nonetheless, no study has yet gathered comprehensive mechanistic evidence.

¹Department of Chemistry, University of Oxford, Oxford, United Kingdom. ²Department of Chemistry, The University of York, York, United Kingdom.

³Present address: School of Nano-Bioscience and Chemical Engineering, Ulsan National Institute of Science and Technology, Ulsan, South Korea.

*e-mail: ben.davis@chem.ox.ac.uk

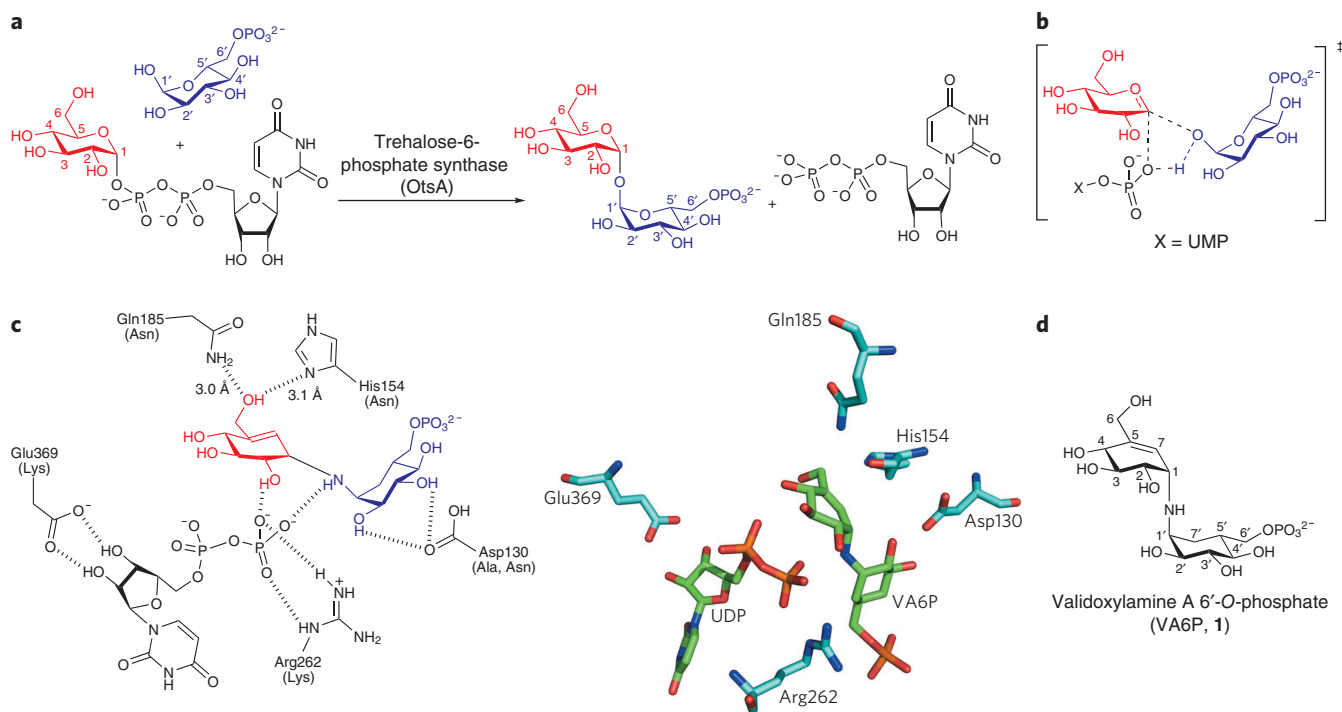


Figure 1 | The reaction catalyzed by trehalose-6-phosphate synthase (OtsA). The numbering shown here corresponds to both VA6P and the product trehalose-6'-phosphate (and the compounds in the main text) to allow consistent numbering through the reaction pathway. Discussion of the nucleotide donor in the main text uses conventional numbering (as shown in **Table 1**); for example, C1 in VA6P corresponds to C1'' in the nucleotide diphosphate donor. **(a)** The reaction forms a glycosidic bond between the OH1'-hydroxyl of acceptor substrate glucose-6-phosphate (blue) and the glucosyl moiety (red) from donor substrate UDP-glucose (UDP-Glc). **(b,c)** The proposed front-face transition state for this reaction **(b)** resembles the complex ternary structure **(c, right)** determined²² for the synergistic binding to OtsA of UDP and validoxylamine A 6'-O-phosphate (VA6P); the corresponding schematic view is also shown **(c, left)**. Each mutation generated for LFER is shown in parentheses in the schematic view. **(d)** The structure of VA6P. Note that the secondary amine in VA6P might be expected to be protonated at physiological pH, but this is not clearly observed (either directly or indirectly) in the determined structures.

The S_Ni -like mechanism involves a front-face nucleophilic attack, thereby leading to net retention in the nucleophilic substitution, which features an open transition state¹⁷. This open transition state is expected to be highly dissociative, with a considerable oxocarbenium ion character¹⁸. An interaction, possibly the formation of hydrogen bonds, between the leaving group and the incoming nucleophile is predicted, which should lead the nucleophile to the same face as the leaving group while assisting leaving group dissociation^{1,17}. Recently, we described the X-ray structure²² of a retaining glycosyltransferase, trehalose-6-phosphate synthase (OtsA), containing uridine diphosphate (UDP) and a bisubstrate analog, validoxylamine A 6'-O-phosphate (VA6P **1**, **Fig. 1d**). OtsA transfers a glucosyl moiety from a donor substrate uridine diphosphate glucose (UDP-Glc) to the 1-hydroxyl group of the acceptor substrate glucose-6-phosphate (Glc6P) to form an α,α -1,1 linkage, yielding the product α,α -1,1-trehalose-6-phosphate (**Fig. 1a**). OtsA belongs to the sequence-based glycosyltransferase 20 (GT20)²³ protein family and possesses a GT-B fold. Kinetically, OtsA uses a sequential ordered bi-bi mechanism in which the donor, UDP-Glc, binds to the active site first, and is followed by the acceptor Glc6P, before the reaction occurs. VA6P shows competitive inhibition with regard to the donor UDP-Glc, and its potency increases considerably in the presence of UDP. This synergistic inhibition is believed to show the plausible geometry and interplay of a leaving group and a nucleophile that can happen in the transition state (**Fig. 1b**). Moreover, the three-dimensional structure of this complex shows that a hydrogen bond exists between the leaving group oxygen of UDP and the nucleophile mimic of the sugar moiety (**Fig. 1c**). This and other structures¹⁵ are consistent

with the suggestions that the S_Ni -like mechanism requires hydrogen bonding that can direct the nucleophile to the same face as the leaving group¹⁷. Computational studies also suggest that hydrogen bonding between the leaving group and the nucleophile contributes to stabilizing the transition state of an S_Ni mechanism¹⁸. Also, the flattened geometry of the leaving group pyranose ring mimic in VA6P is consistent with oxocarbenium ion-like character. Overall, although our previous ternary complex structure is suggestive of an S_Ni mechanism, more experimental data to test the mechanistic hypotheses are required.

In this report, we present what we believe is compelling evidence that observations in our ternary complex reflect true aspects of the transition state. We have probed the characteristics of the putative transition state structure and the participation of the nucleophile in the transition state by means of kinetic isotope effects (KIE) and linear free energy relationships (LFER) on a range of substrates; together these data implicate both the leaving group of the donor and the acceptor nucleophile during the transition state and suggest a front-side, S_Ni -type mechanism.

RESULTS

Confirming transition state mimicry

LFER can be used to probe the sensitivity of reaction rates to electronic factors such as the electronegativity or acidity of atoms near the reaction center²⁴ and can provide a rigorous test of the transition state mimicry of inhibitors²⁵. Using the latter strategy, we compared the effects of identical structural change on the stabilization of the transition state of the reaction (reflected in k_{cat}/K_m) and on the binding affinity of potential transition state mimics (reflected

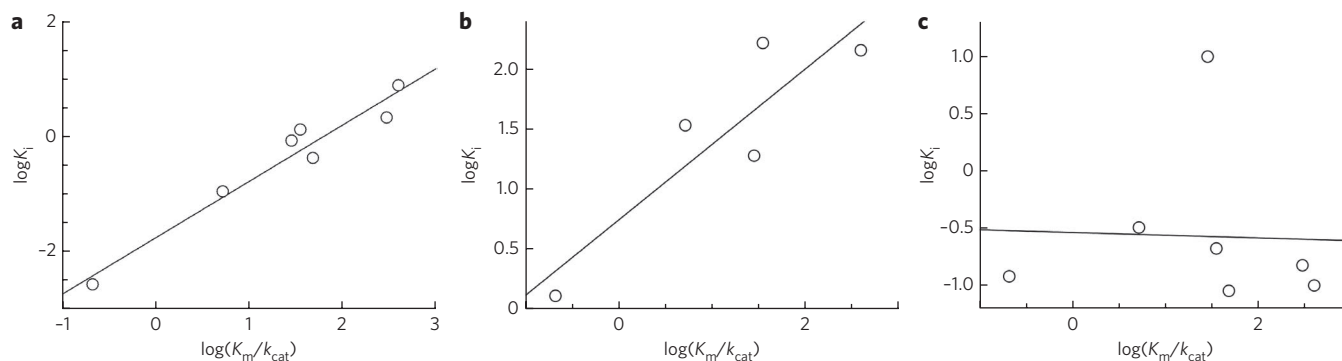


Figure 2 | Linear free energy relationships of OtsA variants. (a) Plot of $\log(K_m/k_{cat})$ of OtsA wild type and mutants versus $\log K_i$ measured with VA6P in the presence of UDP at a concentration of twice the K_i of UDP. The slope is 0.98 ($r^2 = 0.94$), strongly suggesting effective mimicry of the enzyme transition state by the synergistic inhibition of VA6P and UDP. (b) Plot of $\log K_i$ versus $\log(K_m/k_{cat})$ of OtsA wild type and mutants measured with VA6P alone in the absence of UDP. K_i values for two mutants (D130A and D130N) could not be measured as K_i values were very high and out of range of the concentration of VA6P used (up to 160 mM). A weak relationship (slope = 0.63, $r^2 = 0.79$) suggests that VA6P is only a poor transition state mimic in the absence of UDP (or is not a mimic at all). (c) Plot of $\log K_i$ versus $\log(K_m/k_{cat})$ of OtsA wild type and mutants measured with UDP alone in the absence of VA6P. As in b, a lack of correlation suggests that VA6P is not an effective transition state mimic in the absence of VA6P. Three independent measurements were performed for each data point.

in K_i). This can be achieved either by changing the structure of the substrates systematically (giving k_{cat}/K_m values) and of the inhibitors analogously (giving K_i values) or by mutating amino acid residues in the active site of enzymes and measuring both parameters with the same substrate and inhibitor²⁵. Thus, we generated active site mutants of OtsA and measured all relevant kinetic parameters. Initial KIEs observed through k_{cat}/K_m (described below) confirmed that the chemical step was sufficiently isotopically sensitive in the mechanism of OtsA, showing that k_{cat}/K_m reflected the transition state of the chemical reactions, and highlighted this as a highly suitable enzymatic system. To test whether the inhibition by VA6P in the presence of UDP was relevant to the transition state of the reaction, we expressed wild-type and active site-mutant variants of OtsA in *Escherichia coli* and purified them by nickel-affinity chromatography. Kinetic parameters of a donor substrate, UDP-Glc, and an acceptor substrate, Glc6P, were measured by the coupled spectrophotometric assay method²⁶ (Supplementary Table 1).

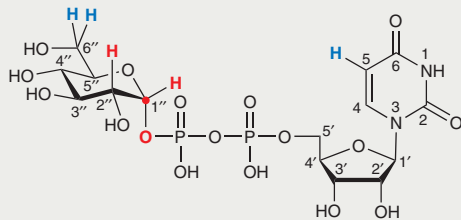
Attempts were made to measure the inhibition constants of VA6P for mutants without UDP. At 5-mM concentrations of VA6P, inhibition was less than 10% with the D130A mutant, and other mutants showed no significant inhibition. Thus, except for the WT enzyme, 5 mM of VA6P alone did not significantly inhibit any mutants, giving determined K_i values that in all cases were at least two orders of magnitude higher than that for the wild type (Supplementary Table 1). Nonetheless, more potent inhibition by VA6P could be measured in the presence of UDP, confirming the synergistic inhibition of VA6P and UDP. First, a radioactivity assay using ³H-labeled UDP-Glc measured inhibition constants of UDP with respect to the donor substrate, UDP-Glc, for the wild-type enzyme and active site variants (described in Methods). Next, a radioactivity assay measured K_i values of VA6P in the presence of UDP. K_i values could be measured with the mutants and ranged from 2.7 μ M for the wild type to 7.6 mM for the least active enzyme mutant, R262K (Supplementary Table 1 and Supplementary Fig. 2). Apparent K_i values of VA6P were measured in the presence of UDP at a concentration corresponding to twice the K_i values of UDP for each mutant. At this concentration of UDP, the occupancy of UDP within the active site was substantial, yet the residual activity was measurable by the sensitive radioactivity assay. Logarithms of K_i values plotted against those of K_m/k_{cat} values revealed a statistically significant relationship with a correlation coefficient (r^2) of 0.94 and a slope of 0.98 (Fig. 2a). Generally, a strong correlation with a slope close to unity is considered to indicate the

meaningful mimicry of transition state²⁵, and therefore this LFER strongly suggested that synergistic inhibitors, VA6P and UDP, formed an *in situ* transition state analog at the active site. VA6P alone gave a very poor correlation (Fig. 2b), and only at high concentrations (>5 mM); UDP alone (Fig. 2c) similarly gave no clear correlation. *In situ* formation of a transition state analog is not rare and is observed in studies of β -phosphoglucomutase²⁷ and a retaining glycosyltransferase, trehalose phosphorylase¹⁹. Consequently, it is likely that the structure of the OtsA ternary complex²² reflects characteristics of the true transition state.

Kinetic analysis of the donor substrate

A powerful method to probe the oxocarbenium ion-like character in the reaction coordinate is through KIEs²⁸. As isotopic change is very sensitive to vibrational mode and frequency, the subtle variation in reaction rate resulting from isotopic substitution provides insight into the changes in bond order and geometry around the atom that is subjected to isotopic substitution while the reaction is going from ground state to the transition state. If the transition state has a looser structure or weaker bonding than the ground state, heavy isotope substitution will result in a slower rate, giving a normal KIE ($k_{light}/k_{heavy} > 1$). In contrast, a transition state with a more constricted environment or stronger bonding between atoms results in a faster rate with heavy isotope substitution, giving an inverse KIE ($k_{light}/k_{heavy} < 1$). Thus, both the mode and magnitude of KIEs can provide detailed information about transition state structure. It is important to note that the reaction coordinate and aspects of reversibility and commitment²⁹ (described below) can also modulate KIE.

We determined multiple KIEs under competitive conditions using the isotopically labeled donor substrates shown in Table 1. These methods used radioisotopes as heavy atoms and remote labels^{30,31} and yielded KIEs based on k_{cat}/K_m ³², which reflected the first irreversible step. Thus, the donor substrate, UDP-Glc, was isotopically labeled at a range of sites with [¹''-³H], [¹''-²H, 5-³H], [²''-²H, 5-³H], [¹''-¹⁴C], [¹''-¹⁸O, 5-³H], [⁶''-³H], [⁶''-¹⁴C] and [⁵-³H] (Table 1). These were synthesized enzymatically or chemoenzymatically from appropriately labeled glucose (Supplementary Methods). As the 6'' position is three bonds away from the reaction center, the KIE from ¹⁴C at this position was assumed to be negligible³³ and was therefore used as a reference. Thus, KIEs of [¹''-³H], [¹''-²H, 5-³H], [²''-²H, 5-³H], [¹''-¹⁸O, 5-³H], [⁶''-³H] and [⁵-³H] measured in pair with [⁶''-¹⁴C] as a competitive light isotopic

Table 1 | Isotopic labels in UDP-Glc and experimental KIEs


Label	Type of KIE	Experimental KIE ^a
1''- ³ H	α-secondary	1.284 (± 0.001)
1''- ² H	α-secondary	1.196 (± 0.003)
1''- ¹⁴ C	Primary label	1.023 (± 0.004) ^b
2''- ² H	β-secondary	1.164 (± 0.003)
1''- ¹⁸ O	Primary; leaving group	1.024 (± 0.002)
6''- ³ H	Remote label	1.049 (± 0.0002)
5- ³ H	Remote label	1.000 (± 0.004)

Shown are the positions of isotopic labels in the donor substrate, UDP-Glc, designed for multiple kinetic isotope effect measurement and the resulting experimental KIEs that were determined. Three to five independent measurements were performed for each KIE, and the data represent mean values ± s.d.
^aMeasured using 2-deoxy-glucose-6-phosphate as an acceptor substrate. ^bCorrected for remote label effect of 6''-³H.

substrate provided a precise internal standard. Similarly, the negligible effect of a [5-³H] label was confirmed and so justified its use as a concomitant silent remote label in [1''-²H, 5-³H], [2''-²H, 5-³H] and [1''-¹⁸O, 5-³H] KIEs. A [1''-¹⁴C] KIE was measured with [6''-³H] labeled substrate as a competitive light isotope label and corrected for remote effects by the latter.

In the retaining glycosyltransferase reaction, the first irreversible step was expected to reflect the departure of a leaving group and the nucleophilic participation of the acceptor nucleophile, as suggested by the LFER through transition state analogy. For KIE to be a meaningful tool for revealing chemical transformation, it is necessary for the chemical step to be the first irreversible step so that the measured KIE is fully intrinsic. Otherwise, measured KIEs will be significantly lower than intrinsic values, confusing the interpretation. Therefore, in many cases it has been necessary to measure commitment factors of the reaction. Commitment factors measure the ratio of the rate of the bond-forming (or bond-breaking) step to the rates of all nonchemical steps, thus revealing how contributory the chemical step is. A correction of experimental KIEs based on measured commitment factors can be made to obtain intrinsic KIEs³². In general, there are two types of commitment factors, forward and reverse. The OtsA-catalyzed reaction is virtually irreversible under the assay conditions, and thus the reverse commitment can be considered zero.

Glc6P was used as an acceptor substrate only for the measurement of a [1''-³H] KIE. Although the [1''-³H] KIE measured with the natural acceptor Glc6P was significantly large (1.205 ± 0.002 s.d.), we also chose the slower and less efficient acceptor substrate, 2-deoxy-D-glucose-6-phosphate (2dGlc6P, **2**) (one-half the k_{cat} and eight-fold higher K_m) to complete our set of multiple KIEs and to make the chemical step more dominant (**Table 1**). Measurement of a full set of KIEs ([1''-³H] and [1''-²H]) with the less active acceptor substrate 2dGlc6P ensured the determination of intrinsic KIEs; indeed, the [1''-³H] KIE of 1.284 obtained using 2dGlc6P was larger than that measured with Glc6P and among the largest reported. Moreover, high K_m values (53 mM, in this case) implicated weak binding and very little commitment³³. Together these data indicated that the KIEs measured with 2dGlc6P can be considered intrinsic.

The α-secondary [1''-³H] KIE was measured to be 1.284. Such large α-secondary ³H (or ²H) KIEs are an indication of oxocarbenium ion-like character at the transition state due to the change of hybridization of anomeric carbon from sp³ to sp², which creates a less restricted environment around the carbon-hydrogen bond, enabling out-of-plane bending freedom of the H(D) atom³⁴. The large β-secondary KIE of [2''-²H], measuring 1.164, further supported this change. The β-secondary deuterium KIE measured the hyperconjugation between the 2''-hydron (either ¹H, ²H or ³H) and the electron-deficient C1'' of the oxocarbenium, which stabilizes the transition state³⁵. This hyperconjugation can be described as electron donation from the sigma bond between H2'' and C2'' to an empty p-orbital of C1'' at the transition state, which results in a weakened C2''-H2'' bond, leading to a normal (>1) KIE. Such electron donation is highly dependent on the torsion angle between C2''-H2'' and the p orbital of C1''. If the pyranose ring is flattened on its way to the transition state, hyperconjugation is more efficient, leading to a large KIE. Together, large normal [1''-³H] KIE and [2''-²H] KIEs (α- and β-secondary, respectively) strongly indicated that the transition state was considerably dissociative, with a substantial oxocarbenium ion-like character, and that the pyranose ring was flattened through C5''-O5''-C1''-C2'' (**Fig. 3**). The [1''-¹⁴C] KIE also supported these observations. [1''-¹⁴C] KIE is a primary effect, normally of magnitude 1.0–1.02 for the transition state of formation of a discrete cationic intermediate (D_N*A_N³⁶), 1.025–1.060 for a dissociative concerted mechanism (A_ND_N), and 1.06–1.16 for an associative or synchronous concerted mechanism (also A_ND_N)^{28,37,38}. Notably, our experimental KIE of 1.023 fell between these value ranges and suggested an intermediate D_N*A_N and dissociative A_ND_N character (**Fig. 3**). This result was consistent with a highly dissociative transition state, but it did not distinguish between the stepwise (D_N*A_N) and concerted (A_ND_N) pathways. Thus, although these experimental ¹⁴C KIE data let us confidently state that the transition state did not have significant bond orders to either the leaving group or the incoming nucleophile, the formation of a discrete oxocarbenium ion intermediate was unclear.

More notable is the leaving group ([1''-¹⁸O]) oxygen KIE, which was determined to be 1.024. This KIE is also primary and, in general, directly proportional to the extent of bond cleavage³⁹. A fully broken carbon-oxygen bond generating an anionic leaving group in glycoside hydrolysis results in a leaving group ¹⁸O KIE of 1.047 (ref. 39). As a comparison, leaving group ¹⁸O KIEs for acid-catalyzed carbon-oxygen bond cleavage presumed to proceed via fully protonated transition states are reported to range from 1.023 to 1.026 (refs. 40,41). These latter measurements suggested that our measured KIE of 1.024 might be consistent with those corresponding to a protonated (at least in part) leaving group oxygen. It should be noted that the previous values were determined using unnatural alkyloxy or aryloxy leaving groups, contrasting with the phosphate leaving group, UDP, that we used. With a phosphate leaving group, negative charge delocalization to or protonation of the nonbridging oxygens may also contribute to the observed lowering of the ¹⁸O leaving group KIE⁴². It may be that protonation and charge delocalization competed for the electron density liberated by the bond cleavage and that the KIE of 1.024 determined here reflected the contributions of both. Partial protonation (which was estimated to be less than 50% from the observation of Brønsted and Taft relationships, described later) appeared also to be consistent with the structure of the ternary complex and with the model that hydrogen bonding between leaving group and nucleophile guides the latter to the same face as the former²². Together, these multiple KIEs were consistent with the observations in the structure of the OtsA ternary complex, its transition state analogy and an S_Ni-like mechanism (**Fig. 4**).

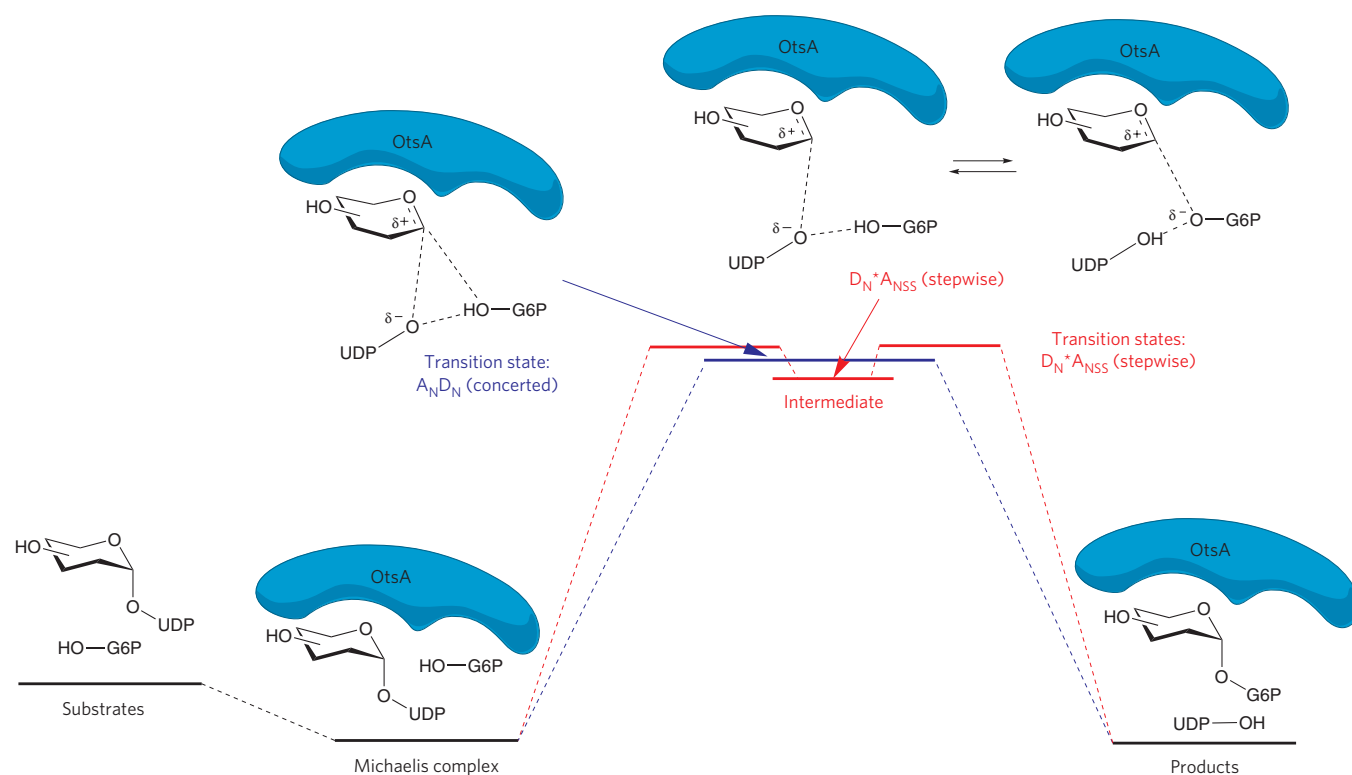


Figure 3 | A schematic diagram depicting the profile (energy versus coordinate) of OtsA-catalyzed reaction. Binding of substrates occurs sequentially (ordered bi-bi), with the donor first, followed by the acceptor. As the reaction reaches the transition state, the following series of events occurs. The leaving group departure is almost completed as the nucleophile starts to form a significant bond. This confers a substantial oxocarbenium ion character on the transition state. Consequently, the pyranose ring of the donor is flattened through C5''-O5''-C1''-C2''. The oxygen atom of the leaving group accepts a hydrogen bond from the nucleophile, and this ensures the presence of the nucleophile along the reaction coordinate. Combined with the Brønsted and Taft-like analyses, these data indicate that the participation of the nucleophile seems to be significant. The mechanism can be either concerted or stepwise. The transition state is highly dissociative in both mechanisms, and the energy difference between the two is expected to be small. If there is a discrete intermediate, the nucleophile contributes to the stabilization of the intermediate.

Kinetic analysis of the acceptor substrate

These results, coupled with transition state analogy, suggested the involvement of both the donor and acceptor substrates; therefore, the participation of acceptor substrates was also probed by LFER studies. We synthesized a panel of modified acceptor substrates: 2-deoxy-D-glucose-6-phosphate (2dGlc6P), 3-deoxy-D-glucose-6-phosphate (**3**), 4-deoxy-D-glucose-6-phosphate (**4**), 2-deoxy-2-fluoro-D-glucose-6-phosphate (2FGlc6P, **5**), 3-deoxy-3-fluoro-D-glucose-6-phosphate (**6**), 4-deoxy-4-fluoro-D-glucose-6-phosphate (**7**) and 2-deoxy-2,2-di-fluoro-D-glucose-6-phosphate (2,2-diFGlc6P, **8**) using hexokinase⁴³ along with the C-2 epimer, 2-deoxy-2-fluoro-D-mannose-6-phosphate (2FMan6P, **9**). Pseudo-single substrate steady-state kinetic experiments tested all eight acceptor substrates (Fig. 4a) in the presence of a saturating concentration of UDP-Glc, and the coupled assay determined kinetic parameters (Supplementary Table 2). All modified substrates showed significant activity. The lowest k_{cat} (2,2-diFGlc6P) was less than that of the natural acceptor by only a factor of 50, and the corresponding k_{cat}/K_m lower by a factor of 200.

The X-ray crystal structure of OtsA complexed with UDP and Glc6P shows that every hydroxyl group of the acceptor makes hydrogen bonds with the enzyme active-site amino acid residues directly or via water molecules⁹. Monodeoxy or monodeoxyfluoro acceptors can be considered to be missing one potential hydrogen bond donor group; this implies that if they are used as acceptors, the penalty given to modified substrates with regard to the loss of binding affinity may be similar. Indeed, K_m values, a rough estimation of enzymatic binding affinity, varied by a factor of less than 2.5

between all our modified substrates, representing just 0.5 kcal mol⁻¹ of apparent binding energy difference. A pertinent example is 2FMan6P, for which the k_{cat} was only slightly higher than that of 2FGlc6P, whereas the K_m was in general agreement (within the error range), thus indicating that the effect of losing one hydrogen bond was approximately identical in both and that the orientation (equatorial or axial) of fluorine substitution had only a minor effect. The natural substrate Glc6P was excluded in all analyses as it has the potential for extra hydrogen bonding, resulting in extra binding energy, which cannot be in line with the desired structure-activity relationships (Supplementary Fig. 3).

First, we performed Brønsted-like analysis. When calculated $\text{p}K_a$ values (Supplementary Table 2 and Supplementary Methods) of the nucleophiles were plotted against $\log(k_{\text{cat}}/K_m)$, it revealed a strong relationship ($r^2 = 0.98$) and a moderate sensitivity of the reaction to nucleophile versus acceptor acidity (slope, $\beta_{\text{nuc}} = 0.54 \pm 0.5$) (Fig. 4b). Second, we conducted Taft-like analysis using acceptors modified only at the C2 position. Again, modification of the substrate at only one position was expected to give more accurate and relevant structure-activity relationships (Fig. 4c). In this analysis, the natural acceptor substrate, Glc6P, was again excluded for the same reasons as in the Brønsted analysis. It should be noted that polar substituent constants for substituents at C-2 of 2dGlc6P, 2FGlc6P, 2,2-diFGlc6P and 2FMan6P are not known, and determined polar substituent constants for CH_3 , CH_2F and CHF_2 were used as the closest approximations⁴⁴. Taft-like analysis gave an excellent correlative relationship ($r^2 = 1.0$) and modest sensitivity (slope, $\rho = -0.62 \pm 0.04$) (Fig. 4c).

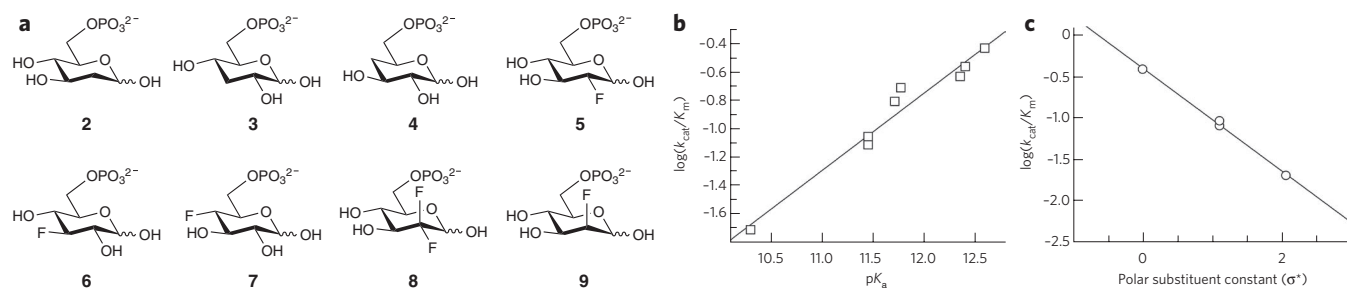


Figure 4 | LFER of acceptor kinetics determined using the varied modified acceptors. (a) Panel of modified deoxy- and deoxyfluoro-acceptor substrates (2–9) of OtsA used to probe the linear free energy relationships of acceptor substrate kinetics. (b) Brønsted relationship of nucleophile basicity and rates. Plot of calculated pK_a of nucleophile versus log(k_{cat}/K_m) (further details are in **Supplementary Methods**). Slope (β_{nuc}) = 0.54, r^2 = 0.98. (c) Taft-like analysis. Plot of polar substituent constants (σ^*) versus log(k_{cat}/K_m). Slope (ρ) = 0.62, r^2 = 1.0. Three independent measurements were performed for each data point.

DISCUSSION

The LFER determined here suggest that synergistic inhibitors, VA6P and UDP, formed an *in situ* transition state analog at the active site of OtsA. Thus, the crystal structure of the ternary complex is likely to reflect the transition state of a retaining glycosyltransferase reaction²². Several conclusions can be drawn from this transition state analogy. First, it suggests that the transition state contains a donor substrate moiety with its leaving group bond largely broken and an acceptor substrate moiety that hydrogen bonds between the leaving group oxygen on UDP and the incoming nucleophile (nitrogen in the crystal structure but oxygen in the native substrate). It can now be seen that this hydrogen bonding is an important feature of the transition state, leading the nucleophile to the same face as the leaving group, as also suggested by a previous computational study¹⁸. Second, we can speculate that the relative distance of the nucleophile might be closer to the anomeric center than that of the leaving group, as the nucleophile-to-carbon bond length is 1.5 Å while the interacting UDP is observed 3.5 Å away from the anomeric center in the structure. Clearly, a carbon-nitrogen covalent bond cannot truly mimic the partial bond nature of a transition state, and indeed an important caveat is that any covalently bonded transition state analogs have to be considered imperfect. Subsequently, the distance between UDP and the anomeric carbon determined from this structure might also be an over- or underestimation. These distances should therefore be taken as a trend of the relative positioning of the leaving group and the nucleophile in the active site. Third, this observed asynchronicity suggested that the oxocarbenium ion-like character is likely featured in the transition state. VA6P has a prearranged flattened anomeric center around C2-C1-O5-C5 of the pyranose ring of the donor mimic. If the reaction proceeded from the ground state to an oxocarbenium ion-like transition state, the geometry of the anomeric center changed from a tetrahedral to a flattened arrangement. This flattened geometry likely contributed to the successful synergistic inhibition of VA6P and UDP as a transition state analog. An oxocarbenium ion-like transition state in the retaining glycosyltransferase reactions was already implicated in earlier studies that attributed the inhibition of retaining glycosyltransferases by UDP-2'-deoxy-2'-fluoro-D-glucose (or corresponding galactose derivative) to the destabilizing effect of an electronegative fluorine adjacent to reaction center on the positively charged transition state^{10,45}. Besides geometry, however, the inhibitor structure formed by VA6P and UDP shows less-than-ideal charge distribution around the putative reaction center as VA6P does not have positive charge on C1 (numbered as shown in Fig. 1 according to VA6P and product trehalose-6'-phosphate; C1 would correspond to C1'' in nucleotide diphosphate donor nomenclature) or C7 (corresponding to endocyclic oxygen O5'' of the donor pyranose ring) that would develop in a transition state. Computational studies on oxocarbenium ion-like transition states of nucleoside glycosylases indicate

that the anomeric carbon assumes the most positive charge²⁸. Logically and elegantly designed inhibitors of glycoside hydrolases and nucleoside glycosylases mimicking this oxocarbenium ion-like transition state incorporate positive charge in these and nearby positions via nitrogen atoms^{28,46}. Strong transition state analogy of the synergistic inhibitors, despite the lack of proper charge distribution, implied that the majority of the stabilization of positive charge at the anomeric carbon of transition state may not be provided by amino acid residues of the enzyme but by the incoming acceptor nucleophile. Indeed, in the case of retaining glycoside hydrolases, it is suggested that the stabilization of a positively charged transition state is largely provided by the enzymatic nucleophile, a carboxylate group of aspartate or glutamate^{1,47}. The LFER determined here are therefore consistent with the lack of an enzymatic nucleophile and indicate that the incoming acceptor nucleophile should play such a role¹. Therefore, it was necessary to further probe the oxocarbenium ion-like character of the transition state and the role of the nucleophile.

All KIEs pointed to a highly dissociative, oxocarbenium ion-like transition state with a flattened pyranose ring (Fig. 3). [1''-¹⁴C] KIE and leaving group [1''-¹⁸O] KIE suggested that the carbon-oxygen bond to the leaving group was almost broken and that there was asymmetric hydrogen bonding or partial protonation of the leaving group oxygen (or possibly delocalization or nonbridging oxygen protonation⁴²) at an early stage. Such hydrogen bonding, or protonation, of the leaving group was again consistent with the observation of hydrogen bonding in the crystal structure of the ternary complex.

Brønsted relationships in our case could be used to expose the trends of the reaction. Here more basic hydroxylate groups for the corresponding conjugate nucleophile hydroxyl were found to accelerate the reaction. This was attributed to the partial deprotonation of the corresponding conjugate hydroxyl group nucleophile at the transition state, which suggested either that deprotonation occurs at an early stage or that the base in question was generally not strong⁴⁸. This was also consistent with the [1''-¹⁸O] KIE observations described above. Together these indicated a partial protonation of the leaving group oxygen where the leaving group is also the general base. The β_{nuc} of 0.55 indicated simultaneous moderate nucleophilic participation, but at this stage, when using calculated pK_a values, it should not be overinterpreted, and assigning a particular value to, for example, bond extension would be premature. Taft-like analysis showed the same trends as Brønsted analysis. Generally, when $0 > \rho > -1$, it is assumed that the reaction is mildly sensitive to the polar effect of the nucleophile. Our Taft analysis, therefore, also suggested nucleophilic participation in the transition state. It cannot be ruled out that the steric bulk of fluorine substitution might also play a role in modulating rates. If this is the case, it can be speculated that the ρ value of -0.62 determined here is a slight overestimation, and a lower dependence

of the reaction on electronic effects would be expected. This would point toward a more dissociative transition state but one that would still involve participation of the nucleophile. Similar to prior studies with internal donor nucleophiles^{49,50}, our results suggested that for retaining glycosyltransferases, the nucleophile stabilizes positive charge on the anomeric carbon at the highly dissociative transition state by virtue of the lone pair electrons of oxygen, not yet making a substantial bond. In this case, the inductive effects observed by us should be read as basicity not as nucleophilicity.

These data combined with the ¹⁸O KIE supported the existence of hydrogen bonding between the leaving group and the acceptor nucleophile. The role of the nucleophile may be to provide the nucleophilic 'push' and the electrostatic stabilization of the cationic anomeric carbon. Also, these LFERs along with the large [1''-¹⁸O] KIE, which should arise from contributions up to and including the first irreversible bond-breaking step, strongly suggested that both the leaving group of the donor and the acceptor nucleophile appear in that transition state. This is not consistent with a double-displacement mechanism.

Individual experimental sets (for example, our LFER data that implicate nucleophile participation) may be interpreted as also being consistent with other mechanisms (for example, KIEs alone do not report on reaction stereochemistry); however, as a whole the complete data seemed to provide a less ambiguous set of conclusions. Within the overall context of all of the results of this report, and structural data (Fig. 1c), we propose that the reaction catalyzed by a retaining glycosyltransferase, OtsA, proceeds via 'same-face' nucleophilic substitution (or S_Ni) involving a transition state that is sufficiently open to allow the approach of the nucleophile, Glc6P, guided by hydrogen bonding from the same face as the leaving group (Fig. 3), as first proposed¹⁷ in nonenzymatic reactions. However, whether this proceeds via a metastable intermediate in the reaction coordinate (stepwise S_Ni D_N*A_{NSS}) or as a concerted mechanism (an extremely dissociative A_ND_N) remains unclear. This study now provides quantitative data for this unusual mechanism. There are few potent inhibitors of glycosyltransferases, despite the breadth of this class of enzymes. Their future design (and any associated therapeutic strategies) might be usefully guided by our findings.

METHODS

OtsA radioactivity-stopped assay. Appropriate concentration of UDP-Glc and Glc6P was prepared in 100 μl of 100 mM HEPES buffer (pH 7.25, 100 mM KCl, 10 mM MgCl₂, 0.1% BSA), as detailed in **Supplementary Methods**. Radioactive UDP-[6-³H]Glc (usually 50,000–150,000 d.p.m.) was added and the reaction mixture was equilibrated at 25 °C. Five microliters of OtsA was added using a syringe to initiate the reaction. After incubation at 25 °C for 3–10 min, the reaction was stopped by heating briefly (30 s) at 80 °C. Four hundred microliters of OtsB (3 units) in 0.05 mM Tris buffer was added to the mixture. OtsB cleaves trehalose-6-phosphate to trehalose to produce the only neutral radioactive product in the mixture. The mixture was further incubated for 1 h at 37 °C, and pH was adjusted to 8.0. The mixture was then loaded onto preconditioned strong anion exchange solid-phase extraction Strata (Phenomenex) cartridge. Flow-through fractions (void volume) and an elution of 100 μl of water were collected in a scintillation counter vial, and 5 ml of liquid scintillation cocktail was added to each vial. Collected solutions were counted by an LS6500 (Beckman-Coulter) liquid scintillation counter. Background samples prepared without OtsA gave no detectable counts.

Kinetic isotope effects. Nonradioactive heavy isotopes such as [1''-²H], [2''-²H] and [1''-¹⁸O] were doubly labeled along with [5-³H]. Consequently, all heavy isotope substrates were ³H-labeled except on one occasion. In the case of [1''-¹⁴C] KIE, KIE was measured with UDP-[1''-¹⁴C]Glc as the heavy isotope substrate and UDP-[6''-³H]Glc as the light isotope substrate, and the observed value was corrected for the remote effect from [6''-³H] ([1''-¹⁴C] KIE = [1''-¹⁴C] KIE (observed) × [6''-³H] KIE).

A master reaction mix was prepared using 2 mM UDP-Glc, 8 mM 2-deoxy-D-glucose-6-phosphate, 50 mM KCl, 10 mM MgCl₂, 3 units of OtsB and 0.1% BSA in 50 mM HEPES buffer (pH 7.2) containing isotopic pairs of radiolabeled UDP-Glc substrates where the ratio of ³H/¹⁴C was approximately 1:1, with an activity of about 100,000 d.p.m. each. The enzymatic reaction was initiated by taking aliquots from the master mix and adding OtsA to each aliquot. The ³H/¹⁴C ratio (or ¹⁴C/³H) from the master mix was measured and taken as R₀. The enzymatic reaction was

incubated at 25 °C and allowed to proceed until 40–50% completed. The reaction was stopped by freezing the mixture with liquid nitrogen. Small aliquots (20 μl) were taken for HPLC analysis of the reaction fraction (f). The unreacted product was purified by HPLC on an UltiMate 3000 System (Dionex) using a Spherisorb SAX anion exchange column (10 × 250 mm, Waters). The column was eluted with a gradient of 15–300 mM ammonium formate (30 min), pH 3.5, and chromatography was monitored by UV detector at 262 nm. The unreacted substrate was eluted at the retention time of 18.5 min and then pooled and lyophilized. The residue was dissolved in 200 μl water and subsequently mixed with 5 ml scintillation cocktail. Liquid scintillation counting was performed on a Liquid Scintillation Counter LS6500 (Beckman-Coulter), preset to read ³H/¹⁴C ratio with a precision of 0.2%. Each counting set was performed for 10 min. Resulting ratios ³H/¹⁴C (or ¹⁴C/³H in the case of [1''-¹⁴C] KIE) were taken as R_t. The reaction fraction was obtained by HPLC analysis comparing the ratio of the peak areas of the substrate UDP-Glc and product UDP with a standard curve measured with a UV detector at 262 nm (column: Waters Spherisorb SAX 4.6 × 250 mm using a gradient of 25–250 mM NaH₂PO₄ for 35 min). KIE was calculated using the following equation

$$\text{KIE} = \frac{\log(1-f)}{\log[(1-f)R_t/R_0]} \quad (1)$$

where f = the fraction reaction (0–1) at time when the reaction was stopped, R_t = ³H/¹⁴C (or ¹⁴C/³H) of unreacted substrate when the reaction was stopped (partial reaction) and R₀ = ³H/¹⁴C (or ¹⁴C/³H) of total substrate (ratio at time zero).

[1''-¹⁸O] KIE was further corrected by percent enrichment of ¹⁸O incorporation by using the following strategy³⁰: the ¹⁸O fraction (0.824) in α-D-glucopyranosyl-[1-¹⁸O]phosphate was taken as its f_{iso} value as this compound as completely converted to the final product [³H]UDP-[1''-¹⁸O]Glc in the enzymatic synthesis.

$$\text{KIE}_{\text{final}} = (\text{KIE}_{\text{measured}} - 1 + f_{\text{iso}}) / f_{\text{iso}} \quad (2)$$

where KIE_{final} = final ¹⁸O KIE, KIE_{measured} = KIE determined by equation (1) and f_{iso} = the percent isotopic fraction of ¹⁸O.

Data fitting and statistics. Kinetic parameters were analyzed through nonlinear regression using either the Michaelis-Menten equation or bisubstrate kinetic equations. All other data were analyzed through linear regression. All data fittings were carried out using GraFit 7.0 (Erithacus Software). Data were typically collected from three individual experiments, and all regressions generated standard errors of means (s.e.m.).

Received 22 December 2010; accepted 10 June 2011; published online 7 August 2011;

References

- Lairson, L.L., Henrissat, B., Davies, G.J. & Withers, S.G. Glycosyltransferases: structures, functions and mechanisms. *Annu. Rev. Biochem.* **77**, 521–555 (2008).
- Kim, S.C., Singh, A.N. & Raushel, F.M. Analysis of the galactosyltransferase reaction by positional isotope exchange and secondary deuterium isotope effects. *Arch. Biochem. Biophys.* **267**, 54–59 (1988).
- Bruner, M. & Horenstein, B.A. Isotope trapping and kinetic isotope effect studies of rat liver α-(2–6)-sialyltransferase. *Biochemistry* **37**, 289–297 (1998).
- Vocadlo, D.J., Davies, G.J., Laine, R. & Withers, S.G. Catalysis by hen egg-white lysozyme proceeds via a covalent intermediate. *Nature* **412**, 835–838 (2001).
- Lairson, L.L. *et al.* Intermediate trapping on a mutant retaining alpha-galactosyltransferase identifies an unexpected aspartate residue. *J. Biol. Chem.* **279**, 28339–28344 (2004).
- Soya, N., Fang, Y., Palcic, M.M. & Klassen, J.S. Trapping and characterization of covalent intermediates of mutant retaining glycosyltransferases. *Glycobiology* **21**, 547–552 (2011).
- Monegal, A. & Planas, A. Chemical rescue of α3-galactosyltransferase. implications in the mechanism of retaining glycosyltransferase. *J. Am. Chem. Soc.* **128**, 16030–16031 (2006).
- Ly, H.D., Loughheed, B., Wakarchuk, W.W. & Withers, S.G. Mechanistic studies of a retaining α-galactosyltransferase from *Neisseria meningitidis*. *Biochemistry* **41**, 5075–5085 (2002).
- Gibson, R.P., Turkenburg, J.P., Charnock, S.J., Lloyd, R. & Davies, G.J. Insights into trehalose synthesis provided by the structure of the retaining glycosyltransferase OtsA. *Chem. Biol.* **9**, 1337–1346 (2002).
- Persson, K. *et al.* Crystal structure of the retaining galactosyltransferase LgtC from *Neisseria meningitidis* in complex with donor and acceptor analogs. *Nat. Struct. Biol.* **8**, 166–175 (2001).
- Gastinel, L.N. *et al.* Bovine α-1,3-galactosyltransferase catalytic domain structure and its relationship with ABO histo-blood group and glycosphingolipid glycosyltransferase. *EMBO J.* **20**, 638–649 (2001).
- Patenaude, S.I. *et al.* The structural basis for specificity in human ABO(H) blood group biosynthesis. *Nat. Struct. Biol.* **9**, 685–690 (2002).

13. Martinez-Fleites, C. *et al.* Insights into the synthesis of lipopolysaccharide and antibiotics through the structures of two retaining glycosyltransferases from family GT4. *Chem. Biol.* **13**, 1143–1152 (2006).
14. Jamaluddin, H., Tumbale, P., Withers, S.G., Acharya, K.R. & Brew, K. Conformational changes induced by binding UDP-2F-galactose to alpha-1,3-galactosyltransferase—implications for catalysis. *J. Mol. Biol.* **369**, 1270–1281 (2007).
15. Vetting, M.W., Frantom, P.A. & Blanchard, J.S. Structural and enzymatic analysis of MshA from *Corynebacterium glutamicum*. *J. Biol. Chem.* **283**, 15834–15844 (2008).
16. Cowdrey, W.A., Hughes, E.D., Ingold, C.K., Masterman, S. & Scott, A.D. 257. Reaction kinetics and the Walden inversion. Part VI. Relation of steric orientation to mechanism in substitutions involving halogen atoms and simple or substituted hydroxyl groups. *J. Chem. Soc.* 1252–1271 (1937).
17. Sinnott, M.L. & Jencks, W.P. Solvolysis of D-glucopyranosyl derivatives in mixtures of ethanol and 2,2,2-trifluoroethanol. *J. Am. Chem. Soc.* **102**, 2026–2032 (1980).
18. Tvaroska, I. Molecular modeling of retaining glycosyltransferases in *NMR Spectroscopy and Computer Modeling of Carbohydrates* (eds. Vliegthart, J.F.G. *et al.*) 285–301 (American Chemical Society, 2006).
19. Nidetzky, B. & Eis, C. α -Retaining glucosyl transfer catalysed by trehalose phosphorylase from *Schizophyllum commune*: mechanistic evidence obtained from steady-state kinetic studies with substrate analogues and inhibitors. *Biochem. J.* **360**, 727–736 (2001).
20. Goeld, C., Griessler, R., Schwarz, A. & Nidetzky, B. Structure-function relationships for *Schizophyllum commune* trehalose phosphorylase and their implications for the catalytic mechanism of family GT-4 glycosyltransferase. *Biochem. J.* **397**, 491–500 (2006).
21. Goeld, C. & Nidetzky, B. Sucrose phosphorylase harboring a redesigned, glycosyltransferase-like active site exhibits retaining glucosyl transfer in the absence of a covalent intermediate. *ChemBioChem* **10**, 2333–2337 (2009).
22. Errey, J.C. *et al.* Mechanistic insight into enzymatic glycosyl transfer with retention of configuration through analysis of glycomimetic inhibitors. *Angew. Chem. Int. Ed. Engl.* **49**, 1234–1237 (2010).
23. Coutinho, P.M., Deleury, E., Davies, G.J. & Henriissat, B. An evolving hierarchical family classification for glycosyltransferases. *J. Mol. Biol.* **328**, 307–317 (2003).
24. Greig, I.R. The analysis of enzymic free energy relationships using kinetic and computational models. *Chem. Soc. Rev.* **39**, 2272–2301 (2010).
25. Mader, M.M. & Bartlett, P.A. Binding energy and catalysis: the implications for transition-state analogs and catalytic antibodies. *Chem. Rev.* **97**, 1281–1302 (1997).
26. Gosselin, S., Alhussaini, M., Streiff, M.B., Takabayashi, K. & Palcic, M.M. A continuous spectrophotometric assay for glycosyltransferases. *Anal. Biochem.* **220**, 92–97 (1994).
27. Baxter, N.J. *et al.* A Trojan horse transition state analogue generated by MgF_3^- formation in an enzyme active site. *Proc. Natl. Acad. Sci. USA* **103**, 14732–14737 (2006).
28. Berti, P.J. & McCann, J.A.B. Toward a detailed understanding of base excision repair enzymes: transition state and mechanistic analyses of N-glycoside hydrolysis and N-glycosyl transfer. *Chem. Rev.* **106**, 506–555 (2006).
29. Northrop, D.B. Minimal kinetic mechanism and general equation for deuterium isotope effects on enzymic reactions: uncertainty in detecting a rate-limiting step. *Biochemistry* **20**, 4056–4061 (1981).
30. Werner, R.M. & Stivers, J.T. Kinetic isotope effects studies of the reaction catalyzed by uracil DNA glycosylase: evidence for an oxocarbenium ion-uracil anion intermediate. *Biochemistry* **39**, 14054–14064 (2000).
31. Luo, M. & Schramm, V.L. Transition state structure of *E. coli* tRNA-specific adenosine deaminase. *J. Am. Chem. Soc.* **130**, 2649–2655 (2008).
32. Cleland, W.W. The use of isotope effects to determine enzyme mechanisms. *Arch. Biochem. Biophys.* **433**, 2–12 (2005).
33. Lee, J.K., Bain, D.A. & Berti, P.J. Probing the transition states of four glucoside hydrolyses with ^{13}C kinetic isotope effects measured at natural abundance by NMR spectroscopy. *J. Am. Chem. Soc.* **126**, 3769–3776 (2004).
34. Glad, S.S. & Jensen, F. Transition state looseness and α -secondary kinetic isotope effects. *J. Am. Chem. Soc.* **119**, 227–232 (1997).
35. Sunko, D.E., Szele, I. & Hehre, W.J. Hyperconjugation and the angular dependence of β -deuterium isotope effects. *J. Am. Chem. Soc.* **99**, 5000–5005 (1977).
36. Guthrie, R.D. & Jencks, W.P. IUPAC recommendations for the representation of reaction mechanisms. *Acc. Chem. Res.* **22**, 343–349 (1989).
37. Huang, X., Tanaka, K.S.E. & Bennet, A.J. Glucosidase-catalyzed hydrolysis of α -D-glucopyranosyl pyridinium salts: kinetic evidence for nucleophilic involvement at the glucosidation transition state. *J. Am. Chem. Soc.* **119**, 11147–11154 (1997).
38. Chan, J., Lewis, A.R., Gilbert, M., Karwaski, M.-F. & Bennet, A.J. A direct NMR method for the measurement of competitive kinetic isotope effects. *Nat. Chem. Biol.* **6**, 405–407 (2010).
39. Rosenberg, S. & Kirsch, J.F. Oxygen-18 leaving group kinetic isotope effects on the hydrolysis of nitrophenyl glycosides. 2. Lysozyme and beta-glucosidase: acid and alkaline hydrolysis. *Biochemistry* **20**, 3196–3204 (1981).
40. Bennet, A.J. & Sinnott, M.L. Complete kinetic isotope effect description of transition states for acid-catalyzed hydrolyses of methyl alpha- and beta-glucopyranosides. *J. Am. Chem. Soc.* **108**, 7287–7294 (1986).
41. Indurugalla, D. & Bennet, A.J. A kinetic isotope effect study on the hydrolysis reactions of methyl xylopyranosides and methyl 5-thioxylopyranosides: oxygen versus sulfur stabilization of carbenium ions. *J. Am. Chem. Soc.* **123**, 10889–10898 (2001).
42. Du, X., Black, G.E., Lecchi, P., Abramson, F.P. & Sprang, S.R. Kinetic isotope effects in Ras-catalyzed GTP hydrolysis: evidence for a loose transition state. *Proc. Natl. Acad. Sci. USA* **101**, 8858–8863 (2004).
43. Chenault, H.K., Mandes, R.F. & Hornberger, K.R. Synthetic utility of yeast hexokinase. Substrate specificity, cofactor regeneration, and product isolation. *J. Org. Chem.* **62**, 331–336 (1997).
44. Hansch, C. & Leo, A. *Substituent Constants for Correlation Analysis in Chemistry and Biology* (John Wiley & Sons, New York, 1979).
45. Gibson, R.P., Tarling, C.A., Roberts, S., Withers, S.G. & Davies, G.J. The donor subsite of trehalose-6-phosphate synthase. *J. Biol. Chem.* **279**, 1950–1955 (2004).
46. Gloster, T.M. & Davies, G.J. Glycosidase inhibition: assessing mimicry of the transition state. *Org. Biomol. Chem.* **8**, 305–320 (2010).
47. Sinnott, M.L. Catalytic mechanism of enzymic glycosyl transfer. *Chem. Rev.* **90**, 1171–1202 (1990).
48. Ye, J.-D., Li, N.-S., Dai, Q. & Piccirilli, J.A. The mechanism of RNA strand scission: an experimental measure of the Bronsted coefficient, β_{nu} . *Angew. Chem. Int. Ed. Engl.* **46**, 3714–3717 (2007).
49. Jones, C.S. & Kosman, D.J. Purification, properties, kinetics, and mechanism of β -N-acetylglucosaminidase from *Aspergillus niger*. *J. Biol. Chem.* **255**, 11861–11869 (1980).
50. Macauley, M.S., Whitworth, G.E., Debowski, A.W., Chin, D. & Vocadlo, D.J. O-GlcNAcase uses substrate-assisted catalysis. *J. Biol. Chem.* **280**, 25313–25322 (2005).

Acknowledgments

We thank the Bill and Melinda Gates Foundation, the Samsung Fellowship and the Biotechnology and Biological Sciences Research Council for financial support. R. Zhang and S.G. Withers (University of British Columbia) are acknowledged for providing 2-deoxy-2,2-difluoroglucose; R. Gibson (currently at the University of Liverpool) is thanked for initial construction of some OtsA mutants. B.G.D. and G.J.D. are both Royal Society Wolfson Research Merit Award recipients, and B.G.D. is supported by an Engineering and Physical Sciences Research Council Life Sciences Interface Platform grant.

Author contributions

S.S.L. and B.G.D. designed the experiments. A.I. provided mutant *otsA* plasmids. S.S.L., S.Y.H. and J.C.E. expressed the mutants. S.S.L. and J.C.E. performed the kinetic measurements. S.S.L. performed all other experiments. S.S.L., B.G.D. and G.J.D. analyzed the experiments. B.G.D., S.S.L. and G.J.D. wrote the manuscript.

Competing financial interests

The authors declare no competing financial interests.

Additional information

Supplementary information and chemical compound information is available online at <http://www.nature.com/naturechemicalbiology/>. Reprints and permissions information is available online at <http://www.nature.com/reprints/index.html>. Correspondence and requests for materials should be addressed to B.G.D.